
Article:
Velez-Aguilera, G., de Dios Gomez-Lopez, J., Jimenez-Gutierrez, G.E. et al. (5 more authors) (2018) Control of nuclear beta-dystroglycan content is crucial for the maintenance of nuclear envelope integrity and function. Biochimica et Biophysica Acta (BBA) - Molecular Cell Research, 1865 (2). pp. 406-420. ISSN 0167-4889

https://doi.org/10.1016/j.bbamcr.2017.11.013

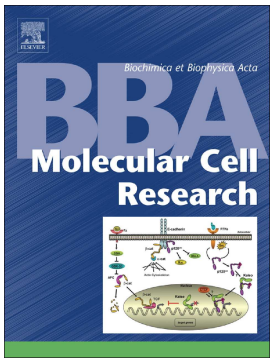

Control of nuclear β-dystroglycan content is crucial for the maintenance of nuclear envelope integrity and function

Griselda Vélez-Aguilera, Juan de Dios Gómez-López, Guadalupe E. Jiménez-Gutiérrez, Alejandra Vásquez-Limeta, Marco S. Laredo-Cisneros, Pablo Gómez, Steve J. Winder, Bulmaro Cisneros

PII: S0167-4889(17)30312-9
DOI: doi:10.1016/j.bbamcr.2017.11.013
Reference: BBAMCR 18216

To appear in:

Received date: 4 August 2017
Revised date: 7 November 2017
Accepted date: 20 November 2017

Please cite this article as: Griselda Vélez-Aguilera, Juan de Dios Gómez-López, Guadalupe E. Jiménez-Gutiérrez, Alejandra Vásquez-Limeta, Marco S. Laredo-Cisneros, Pablo Gómez, Steve J. Winder, Bulmaro Cisneros , Control of nuclear β-dystroglycan content is crucial for the maintenance of nuclear envelope integrity and function. The address for the corresponding author was captured as affiliation for all authors. Please check if appropriate. Bbamcr(2017), doi:10.1016/j.bbamcr.2017.11.013

Control of nuclear β-dystroglycan content is crucial for the maintenance of nuclear envelope integrity and function

Griselda Vélez-Aguilera[1]; Juan de Dios Gómez-López[1]; Guadalupe E. Jiménez-Gutiérrez[1]; Alejandra Vásquez-Limeta[1,2]; Marco S. Laredo-Cisneros[1]; Pablo Gómez[1]; Steve J. Winder[3] and Bulmaro Cisneros*[1]

[1]Departamento de Genética y Biología Molecular, Centro de Investigación y de Estudios Avanzados del Instituto Politécnico Nacional (CINVESTAV-IPN), Mexico City, Mexico.
[2]Laboratory of Protein Dynamics and Signaling, Center for Cancer Research-Frederick, National Cancer Institute, National Institutes of Health, Frederick, MD 21702.
[3]Department of Biomedical Science, University of Sheffield, Western Bank, Sheffield S10 2TN, United Kingdom.

* Correspondence to: B. Cisneros, CINVESTAV-IPN, Departamento de Genética y Biología Molecular. Av. Instituto Poloitécnico Nacional 2508, San Pedro Zacatenco, Gustavo A. Madero, 07360 Mexico City, Mexico. Tel.: +52 55 5061 3339; fax: +52 55 5061 3931.
E-mail: bcisnero@cinvestav.mx

Author Contributions

BC and GVA: Conceived and designed the experiments. GVA, JDDGL, GEJG, AVL, MSLC and PG: Performed the experiments. BC, GVA, JDDGL, GEJG, AVL and MSLC: Analysed data. BC and SJW: Contributed reagents/material/analysis tools. BC, GVA and SJW: Wrote the paper.

Funding

This work was supported by Consejo Nacional de Ciencia y Tecnología, a grant to BC (237123).

Competing interests

The authors declare no competing interests.

ABSTRACT

β-dystroglycan (β-DG) is a plasma membrane protein that has ability to target to the nuclear envelope (NE) to maintain nuclear architecture. Nevertheless, mechanisms controlling β-DG nuclear localization and the physiological consequences of a failure of trafficking are largely unknown. We show that β-DG has a nuclear export pathway in myoblasts that depends on the recognition of a nuclear export signal located in its transmembrane domain, by CRM1. Remarkably, NES mutations forced β-DG nuclear accumulation resulting in mislocalization and decreased levels of emerin and lamin B1 and disruption of various nuclear processes in which emerin (centrosome-nucleus linkage and β-catenin transcriptional activity) and lamin B1 (cell cycle progression and nucleoli structure) are critically involved. In addition to nuclear export, the lifespan of nuclear β-DG is restricted by its nuclear proteasomal degradation. Collectively our data show that control of nuclear β-DG content by the combination of CRM1 nuclear export and nuclear proteasome pathways is physiologically relevant to preserve proper NE structure and activity.

Keywords: β-dystroglycan**,** exportin CRM1, nuclear export, nuclear envelope, proteasome degradation.

Abbreviations

β-DG Beta-dystroglycan
CRM1 Chromosomal Maintenance 1
NES Nuclear Export Signal
LMB Leptomycin B
NE Nuclear Envelope

1. INTRODUCTION

Dystroglycan (DG) is a central component of the dystrophin associated protein complex (DAPC), a multimeric protein assembly that functionally connects the extracellular matrix to the actin-based cytoskeleton [1] DG is post-translationally cleaved into the extracellular α-DG subunit and the transmembrane β-DG subunit (reviewed in [2]). α-DG acts as a receptor for several extracellular matrix proteins, including laminin and other lamin G (LG) module-containing proteins, while β-DG functions as a platform for different adhesion-related processes, including cytoskeleton remodeling [3, 4], extracellular signal-related kinase mitogen-activated protein kinase (ERK-MAPK) signaling [5], and controlling the dynamics of cellular adhesions in myoblasts [6].

The recently unveiled nuclear localization of β-DG expands the diversity of recognized functions of this protein; β-DG is translocated to the nucleus in an importin (IMP) α2/β1-dependent fashion, through recognition of a nuclear localization signal (NLS) located in its juxtamembrane region [7, 8]. Nuclear β-DG in turn interacts with the nuclear envelope (NE) proteins emerin and lamins A/C and B1, which enables it to modulate NE structure and function in myoblasts [9]. Thus, the broad range of localizations and mechanisms in which β-DG is involved implies that trafficking of the protein may be tightly regulated to attain proper subcellular distribution in response to specific stimuli. Since β-DG localizes to both plasma membrane and NE, we envisaged that β-DG might have a functional nuclear export pathway that acts in coordination with the IMPα2/β1-mediated nuclear import to control cellular destination and regulate the concentration of the protein in each cell compartment.

In this study we show for the first time that there is an exportin1/Chromosome Region Maintenance 1 (CRM1)-mediated nuclear export pathway that regulates the ability of β-DG to exit the nucleus via the recognition of a nuclear export signal (NES) located in the transmembrane domain of β-DG. Remarkably, we demonstrated that abnormal nuclear accumulation of β-DG alters both targeting at the NE and the proteins levels of lamin B1 and emerin, which in turn impairs various crucial cellular processes regulated by these two proteins. In summary, our data show that the combination of CRM1-dependent nuclear export and nuclear proteasome pathways prevent harmful nuclear accumulation of β-DG, and consequently these mechanisms are physiologically relevant for proper NE organization and activity.

2. MATERIAL AND METHODS

2.1. Cell culturing, treatments, and transfection

Mouse C2C12 myoblasts were acquired from ATCC, and grown as previously [9]. Mouse primary myoblasts were isolated and cultured as previously described [10]. For inhibition of nuclear protein export, myoblasts were treated for 5 h with 50 nM of Leptomycin B (LMB; Sigma-Aldrich, St Louis), diluted in ethanol 70% or with ethanol alone. For analysis of β-DG stability, cells treated with ethanol (vehicle) or LMB as above were incubated with 30 µg/ml cycloheximide (CHX) (Sigma-Aldrich, St Louis) to inhibit protein synthesis. Cells were harvested at 0, 12, 24 and 30 h of CHX treatment for further analysis. The proteasome inhibitor MG132 (Sigma-Aldrich, St Louis), was used at 10 µM for 30 h. For transfection, C2C12 myoblasts seeded onto glass coverslips were incubated overnight prior to being transfected with 3 µg of the appropriate vector premixed with 3 µl of Lipofectamine 2000 (Invitrogen, Carlsbad, CA, USA), following the supplier's protocol, and were analyzed 24 h post-transfection. For knockdown experiments, C2C12 cells were stably expressing with psi-mH1 vector expressing a small interfering RNA (RNAi) specific for mouse CRM1, with a scrambled RNAi as a control (GeneCopoeia, Inc., Rockville, MD). Stably-transfected C2C12 myoblasts were obtained by culturing them for 12 days in the presence of 2 µg/ml Puromycin (Invitrogen), prior to being used for further experiments.

2.2. Immunofluorescence and confocal microscopy analysis

Immunofluorescence assays were carried out as previously [11], and cell preparations were analyzed on a confocal laser scanning microscope (TCS-SP2, Leica, Heidelberg, Germany), using a Plan Neo Fluor 63x (NA = 1.4) oil-immersion objective. Single optical sections were visualized to analyze colocalization between fluorescent markers. Analysis of digitized images were carried out using Fiji software [12] to determine the nuclear to cytoplasmic ratio (Fn/c), and nucleoli volume and 3D reconstruction.

2.3. Plasmids and antibodies

The eukaryotic expression vectors encoding GFP and GFP-β-DG were previously described [7]. The mutant derivative GFP-β-DGNESm, which contains three-point mutations in the NES motif of β-DG at I763A/L764A/L765A positions, was generated by standard site-directed mutagenesis techniques, using GFP-β-DG vector as the template, the high fidelity Herculase II Fusion DNA polymerase (Agilent Technologies, Santa Clara, CA), and the following oligonucleotides: forward 5'-GGTCGCGGCC**GC**C**GC**G**GC**CAT TGCTGGAATC-3' and reverse 5'-GATTCCAGC-

AATG**GC**C**GC**G**GC**GGCCGCGACC-3'. Vectors expressing GFP in frame with the NES motif of β-DG and the retroviral protein REV were engineered using the following oligonucleotides: for GFP-NESβ-DG forward 5'-GATCCAATCCTGCTCATTGC-TGGCATCATTGCCATG-3' and reverse 5'-GATCCATGGCAATGATGCCAGCAATGAG-CAG-GATTG-3' flanked by EcoR1 and BglII sites respectively; for GFP-NESREV forward 5'-AATTCGCTACCACCGCTTGAGAGACTTACTCTTTAAG-3' and reverse 5'-TCGACTT-AAAGAGTAAGTCTCTCAAGCGGTGGTAGCG-3', flanked by SalI and EcoRI sites respectively. Annealed oligonucleotides for NES-β-DG and NESREV were cloned in frame into pQBI and pEGFP-C1 respectively, via standard restriction/ligation techniques. Vectors encoding Glutathione S-transferase (GST) alone or fused to β-DG were previously described [9]. For knockdown experiments, psi-mH1 vector expressing either a small interfering RNA (RNAi) specific for mouse exportin1/CRM1 CRM1 or a scrambled RNAi control was acquired from GeneCopoeia, Inc. (Rockville, MD). All constructs were confirmed by DNA sequencing.

The following primary antibodies were used: rabbit polyclonal (JAF) [13], rabbit polyclonal (Dystroglycan [p Tyr892]) [14] , goat polyclonal (C20), and mouse monoclonal (MANDAG2) [15] or (7D11) [Santa Cruz Biotechnology, CA] anti-β-DG antibodies. Rabbit polyclonal antibodies directed against GFP (FL), calnexin (H70), emerin (FL-254), lamin A/C (H-110), Sp3 (D-20), [Santa Cruz Biotechnology, CA, USA]; fibrillarin (ab5821), lamin B1 (ab16048) [Abcam, Cambridge, UK]; CRM1 (NB100-79802) [Novus Biologicals, Littleton, CO]. Mouse monoclonal antibodies directed against GST (B-14), GAPDH (6C5) [Santa Cruz Biotechnology, CA, USA]; lamin A/C (ab8984) [Abcam, Cambridge, UK]; ϒ-tubulin (GTU-88) [Sigma-Aldrich] and actin (a gift from Dr. Manuel Hernández, CINVESTAV-IPN, Mexico).

2.4. Cell fractionation

To obtain cytosolic and nuclear lysates, cells were collected by centrifugation at 3,500g for 15 min at 4ºC, and resuspended in 1 ml TM buffer (10 mM Tris-HCl pH 8.0, 2 mM $MgCl_2$, 0.5 mM PMSF), containing 1X complete protease and phosphatase inhibitors (2 mM Na_3VO_4, 10 mM Na_2MoO_4, and 25 mM NaF), and further incubated for 10 min on ice. To solubilize the homogenates, 2% Triton X-100/PBS was added to obtain 1% Triton X-100 final concentration, prior to incubation for 10 min on ice. Nuclei were separated from the cytosolic membranes using a glass Dounce homogenizer (30 strokes using the B pestle) and centrifuged at 3,500g for 15 min at 4ºC. The integrity of the nuclei without debris or cytoplasmic membranes was verified by observation under the light microscope. The supernatant containing the cytosolic fraction was separated, and the nuclear pellet was resuspended in 1 ml of buffer I (0.32 M Sucrose, 3 mM $CaCl_2$,

2 mM $Mg(COO)_2$, 0.1 mM EDTA, 10 mM Tris-HCl pH 8.0, 1 mM DTT, 0.5 mM PMSF, 0.5% (v/v) NP40) and 1 ml of buffer II (2 M Sucrose, 2 mM $Mg(COO)_2$, 0.1 mM EDTA, 10 mM Tris-HCl pH 8.0, 1 mM DTT, 0.5 mM PMSF), and further purified by centrifugation at 45,000g through a sucrose gradient for 1 h at 4ºC. Nuclei were recovered using lysis buffer (50 mM Tris-HCl pH 8.0, 150 mM NaCl, 1 mM PMSF, 1% (v/v) Triton X-100), supplemented with protease inhibitor cocktail and phosphatase inhibitors, vortexed for 30 min at 4ºC, sonicated at 4 microns for 2 min and pre-cleared at 18,000g for 2 min at 4ºC. The nuclear envelope (NE) fraction was obtained as previously [11, 16, 17]. Briefly, purified nuclei were resuspended in 1 ml of ice-cold 10% STM buffer [10% sucrose (w/v), 50 mM Tris–HCl pH 8.5, 0.1 mM $MgCl_2$, 1 mM DTT, 1X complete (Roche Applied Science) and 0.5 mM PMSF]. Then chromatin was digested with 50 U/ml DNase I (Sigma–Aldrich) and 5 µg/ml RNase A (Sigma–Aldrich) for 1h on ice. Next, 4 ml of extraction buffer [10% sucrose (w/v), 50 mM Tris–HCl pH 8.5, 0.1 mM MgCl2, 1 mM DTT, 1X complete (Roche Applied Science) and 0.5 mM PMSF] were added drop-wise. The suspension was underlayed with 4 ml of ice-cold sucrose cushion [30% sucrose (w/v), 50 mM Tris–HCl pH 7.5, 0.1 mM MgCl2, 1mMDTT, 1X Complete (Roche Applied Science) and 0.5mM PMSF] and centrifuged at 4,000g for 15 min in a swinging bucket rotor. The pellet was resuspended in 1 ml of ice-cold extraction buffer including 0.3 mg/ml of heparin, and incubated at 4°C for 1 h. The suspension was underlayed again with 4 ml of ice-cold sucrose cushion and centrifuged as above. The resulting pellet that correspond to the NE was resuspended in RIPA 1X buffer. The nucleoplasmic fraction, was obtained as previously [18], purified nuclei were resuspended in 1 ml of ice cold 10% STM buffer and spun 2,000g for 15 min. The pellet was then resuspended in 2ml of hypotonic buffer [20mM HEPES pH 7.9, 5mM KCl, 1.5Mm DTT, 1X complete (Roche Applied Science) and 0.5 mM PMSF] and homogenization was performed by applying 20 strokes with a Dounce homogenizer. Nuclear homogenates were centrifuged at 6,300g for 15 min at 4ºC. The resulting pellet was resuspended in 2 ml of ice-cold extraction buffer and centrifuged at 100,000g for 45 min. The supernatant that correspond to the nucleoplasm (soluble nuclear protein) extract was collected.

2.5. Immunoprecipitation and GST binding assay

GFP-based immunoprecipitation was performed using 500 µg of C2C12 cell lysates and the GFP-Trap® bead system (Chromotek, Planegg, Germany), and following the manufacturer's instructions. GST-based pull-down assays were performed as previously described [19]. Briefly, an aliquot (20 ml) of transformed bacterial cells (strain BL21), induced with 0.1 mM IPTG for 2 h at room temperature, then were centrifuged at 2,000g for 10 min, resuspended in 1 ml of NETN buffer

[100 mM (w/v) NaCl, 20 mM (w/v) Tris-HCl (pH 7.5), 1 mM (w/v) EDTA, 0.5% (v/v) NP40, 1 mM (w/v) PMSF, 0.5% (w/v), complete protease inhibitor cocktail] and sonicated on ice (4 x 30 s, Branson sonifier). GST, GST-β-DG and GST-Multi-MDSK [20] recombinant proteins were affinity purified using glutathione-Sepharose 4B beads (Amersham Biosciences Co., Piscataway, NJ). To perform pull-down assays, similar amounts of the recombinant proteins immobilized onto 20 µl of glutathione-Sepahrose beads, were incubated for 2h at 4°C on a rotator with 0.5 mg of C2C12 cell extract. Beads were recovered by centrifugation at 2, 000g for 5 min and washed 4 times with 0.5 ml ice-cold NETN buffer. Eluted proteins were subjected to SDS-PAGE and the interacting proteins were identified by western blotting analysis, using the appropriate primary antibodies.

2.6. Western blotting

Cell lysates were subjected to electrophoresis on 10% SDS-polyacrylamide gels and transferred onto nitrocellulose membranes (Hybond-Nþ, Amersham Pharmacia, GE Healthcare, Buckinghamshire, UK). Membranes were blocked in TBST [100 mM Tris-HCl pH 8.0, 150 mM NaCl, 0.5% (v/v) Tween-20] with 5% low-fat dried milk and then incubated overnight at 4°C with the appropriate primary antibodies. Specific proteins were visualized using enhanced chemiluminescence (ECL™) western blotting detection system (Amersham Pharmacia, GE Healthcare), following manufacturer's instructions.

2.7. Total RNA extraction and Quantitative reverse transcription PCR (RT-qPCR)

Total RNA was isolated from C2C12 myoblasts stably-expressing GFP, GFP-β-DG or GFP- β-DGNESm recombinant protein, using the Direct-zol™RNA MiniPrep kit according to the manufacturer's instructions (Zymo Research, Irvine CA). Real time quantitative reverse transcription-PCR was carried on the Step One Plus Real Time PCR System (Applied Biosystems, Foster CA), using 100 ng of total RNA and the KAPA SYBR Fast One Step qRT-PCR system (KAPABIOSYSTEMS; Wilmington MA) and its standard protocol for qPCR cycling. The expression levels of emerin, lamin B1, lamin A and lamin C mRNA were quantified by the $2^{\Delta\Delta ct}$ method, normalized to GAPDH. Primer sequences were as follow: lamin B1 forward 5'-CTTGAGAATGCCAGACTCTC-3' and reverse 5'-AAACACGCTCTAGACTCTTT-3'; emerin forward 5'-CAACTCGTCATCTTCT-TCATTCTC-3' and reverse 5'-GTCATCATTATAGTCCTTGCTCTG-3'; lamin A forward 5'-TCCACTGGAGAAGAAGTGGC-3' and reverse 5'-GTGAGCGCAGGTTGTACTCAG-3'; lamin C forward (the same lamin A

forward primer) and reverse 5'-CTGCCACTCACACGGTGGTG-3'; and GAPDH forward 5'-CTTGGGCTACACTGAGGACC-3' and reverse 5'-CTGTTGCTGTAGCCGTATTC-3'.

2.8. Proliferation assay

Cells stably expressing GFP, GFP-β-DG or GFP-β-DGNESm were harvested and plated in triplicate onto 12 wells microplates at 1 x 10^2 cells/mL confluence. Cell proliferation was assessed for 13 days using the MTT [3-(4,5-dimethylthiazole)- 2-5-diphenyl tetrazolium bromide] commercial kit (Sigma-Aldrich) and following the manufacturer's instructions.

2.9. Flow cytometry

Cells were released from the culture dish using trypsin, followed by pelleting and washing twice with PBS. Cells were then fixed with 80% ethanol for 2 hours, stained for DNA with 1 μg/mL DAPI (Sigma-Aldrich) for 20 minutes and transferred to flow cytometry tubes for cell cycle analysis in a BD LSR-Fortessa flow cytometer (BD Biosciences, San Jose, CA). Cell cycle analysis was carried out using the ModFit LT software (Verity Software House, Topsham, ME).

To synchronize cells in G0/G1 phase, cells stably expressing GFP, GFP-β-DG or GFP-β-DGNESm were cultured in p70 dishes until 80% confluency, then the culture medium was replaced with DMEM medium with a low dose of serum (0.1% FBS) for 48 h. Cells were released from G0/G1 by reconstituting the culture medium with normal sera concentrations. Then, cells were harvested at 0, 12, 19, 21 and 24 h for analysis. To synchronize cells in G1/S-phase. Cells stably expressing GFP, GFP-β-DG or GFP-β-DGNESm were grown in p70 dishes until 60% confluency and incubated with 2 mM thymidine (Sigma-Aldrich) for 18 h. Cells were released from S phase arrest by replacing the culture medium. Then, cells were harvested at 0, 2, 3, 4, 5, 6 and 7 h for analysis. To synchronize cells in late G1/early S a double thymidine block was used. Cells were grown grown in p70 dishes until 60% confluency and incubated with 2 mM thymidine (Sigma-Aldrich) for 18 h, followed by washing and releasing cells into fresh medium for 9 h and were transfected with GFP, GFP-β-DG or GFP-β-DGNESm 4 h post-released then were incubated with 2 mM thymidine for another 18 h and released by replacing the culture medium. Then cells were harvested at 4 h for nucleoli analysis.

2.10. *β*-Catenin activity measurements

C2C12 myoblasts were seeded onto 24 well plates (3 x 10^4 cells/well) and the next day transfected with 0.5 µg of either pEGFP, pEGFP-β-DG or pEGFP-β-DGNESm. Samples were cotransfected with 0.01 µg of TK Renilla luciferase (to estimate transfection efficiency), 0.5 µg of pβ-Catenin and 0.2 µg of either pTOPFLASH or pFOPFLASH (Upstate Biotechnology, Lake Placid, NY). After 24 h, the levels of luciferase and Renilla luciferase were determined in a luminometer using the Dual Luciferase Reporter Assay kit (Promega, Madison, WI). Luciferase activity was normalized to Renilla luciferase activity to adjust for transfection efficiency.

2.11.Statistical analysis

Statistical analyses were performed by the two tailed unpaired Student's t test with Welch's correction, using GraphPad Prism 6 software (La Jolla California USA, www.graphpad.com). Data represent the mean +/- SEM from a series of three or four separate independent experiments and P values < 0.05 are indicative of statistical significance.

3. RESULTS

3.1. *β*-DG can shuttle between the nucleus and cytoplasm

Since β-DG is distributed in both nuclear and non-nuclear fractions, it seems likely that it may be a nucleocytoplasmic shuttling protein with a functional nuclear export pathway. To assess whether β-DG possess an exportin 1/CRM1-dependent nuclear export mechanism, the effect of the exportin CRM1-specific inhibitor leptomycin B (LMB) [21] on the subcellular distribution of β-DG was evaluated in C2C12 myoblasts by confocal laser scanning microscopy (CLSM), using two different antibodies directed against the C-terminal domain of β-DG: 7D11 (mouse monoclonal antibody) and pTyr892 (rabbit polyclonal antibody that specifically recognizes β-DG phosphorylated at Tyr^{892}). The effectiveness of LMB treatment was tested using the classical NES of the human immunodeficiency virus (HIV) type 1 Rev protein fused to GFP (GFP-Rev-NES) as positive control. As expected, GFP-Rev-NES was shifted from the cytoplasm to the nucleus in response to LMB treatment (Figure 1A), confirming that CRM1-mediated nuclear export was effectively blocked. We observed striking accumulation of β-DG in the nucleus upon LMB treatment, using either of the two anti-β-DG antibodies (Figure 1B). When cells were incubated with anti-rabbit or

anti-mouse secondary antibody alone no signal was detected (Supplemental Figure 1), confirming the specificity of anti-β-DG antibodies. Similarly, ectopically expressed GFP-β-DG fusion protein accumulated in the nucleus to a significantly greater extent in LMB-treated cells than in control cells (Figure 1C), with nuclear/cytoplasmic fluorescence ratios (Fn/c) of 2.5 and 1.0 respectively (lower panel). Fluorescence labeling to ascertain whether nuclear export is a natural regulatory mechanism of β-DG rather than a specific process related to immortalization of C2C12 myoblasts, the subcellular distribution of β-DG was also analyzed in mouse primary myoblasts before and after LMB treatment. As expected, β-DG clearly accumulated in the nucleus of primary myoblasts in response to LMB (Figure 1D), with Fn/c values of 1.3 and 2.4 for control and LMB-treated cells respectively (lower panel). Overall these results are consistent with the idea that both β-DG and its Y892 phosphorylated form undergo a CRM1-mediated nuclear export in myoblasts.

3.2. *Nuclear export of β*-DG is mediated by a CRM1-recognized NES located in its transmembrane domain

CRM1-recognised nuclear export signals (NES) generally include 4 or more closely spaced hydrophobic residues, often leucines [22, 23]; the primary amino acid sequence of β-DG was analyzed in an attempt to identify a molecular signal responsible for nuclear export of β-DG, using the NetNES 1.1 Server [24]. This analysis revealed a putative NES located in the transmembrane domain of β-DG [25], within residues ^{763}I LL I AG I IAM^{772} (Figure 2A). The motif exhibits certain conservation among the orthologous proteins from different species (Figure 2A), implying that the nuclear export property of β-DG might be preserved through evolution. To assess NES functionality, we fused the NES of β-DG to the heterologous protein GFP (see Methods), and ascertained whether the NES motif alone is able to mediate nuclear export of GFP. C2C12 myoblasts were transiently transfected to express GFP-NESβ-DG or GFP alone as control (Figure 2B), and the distribution of the fluorescent reporter proteins was examined by CLSM. GFP alone distributed between the cytoplasm and the nucleus, with a comparatively higher signal in the nucleus, and this localization was unchanged after LMB treatment (Figure 2C), with Fn/c of 1.5 and 1.48 for control and LMB-treated cells respectively (right panel). By contrast, GFP-NESβ-DG distributed evenly between the cytoplasm and the nucleus, but was more concentrated in the nucleus upon LMB treatment (Figure 2C), with Fn/c ratios of 1.0 and 1.5 respectively (right panel). These results imply that inclusion of the putative β-DG NES motif was sufficient to confer upon GFP the ability to undergo nuclear export, and that this trafficking pathway is sensitive to LMB.

Hydrophobic residues within the NES are required for protein export. Therefore, in order to identify key hydrophobic amino acids in the NES of β-DG, we generated a three-residue mutant (I763A/L764A/L765A) in the context of full-length β-DG fused to GFP. Afterwards, C2C12 myoblasts were transiently transfected to express GFP-β-DG or the mutant variant GFP-β-DGNESm (Figure 2D), and the distribution of fluorescent recombinant proteins was analyzed by CLSM. Strikingly, and in strong contrast to the even distribution of GFP-β-DG between the cytoplasm and nucleus, the NES mutant variant displayed significantly greater nuclear accumulation (Figure 2E), with Fn/c ratios of 1.0 and 2.5 respectively (right panel): The clear implication of these data is that triple mutation on the hydrophobic residues makes the NES unable to be recognized by the exportin CRM1. As LMB treatment failed to further increase the nuclear localization of GFP-β-DGNESm (Figure 2E), it appears that NES located in the transmembrane domain is the sole or major motif for nuclear export of β-DG.

To directly demonstrate an interaction of β-DG with exportin1/CRM1, in vitro pull-down assays were carried out, whereby GST and GST-β-DG recombinant proteins were expressed in E. coli (Figure 3A, top panel), purified and immobilised on Sepharose prior to incubation with C2C12 total lysates and subsequent WB analysis. Consistent with CLSM data, CRM1 was found to bind GST-β-DG but not GST alone (bottom panel), implying the specificity of the interaction. To confirm that β-DG binds exportin1/CRM1 in a physiological context and that such interactions occurs through the NES, we performed immunoprecipitation assays in intact cells using a GFP-Trap approach. GFP-β-DG but not GFP alone immunoprecipitated endogenous CRM1 from lysates of transiently transfected C2C12 cells, and importantly, GFP-β-DGNESm, which is impaired in nuclear export (see Figure 2C), was unable to interact with CRM1 (Figure 3B). Overall these data imply that CRM1 is the nuclear export transporter for β-DG in living cells and that a NES located in the TM domain of β-DG, mutated in GFP-β-DGNESm, is the target of CRM1.

To further demonstrate the dependence of β-DG nuclear export on exportin-CRM1, we analyzed the impact of exportin 1/CRM1 knockdown on β-DG subcellular localization. To this end, C2C12 myoblasts were transfected with a vector expressing small interfering RNA (RNAi) designed to target CRM1 mRNA or a scrambled RNAi that is predicted not to block the expression of any specific gene, as negative control. WB analysis of lysates obtained from cells stably expressing each RNAi (Figure 3C), and the subsequent quantitative analysis (bottom panel) showed that the CRM1 RNAi was effective in depleting exportin CRM1 protein levels, resulting in a decrease of 70%. It is worth to note that knockdown of CRM1 may affect nuclear export of over 230 identified cargos [26], with unpredictable consequences to cell physiology. We found β-DG to accumulate in

the nucleus of CRM1-depleted cells to a greater extent than control RNAi cells (Figure 3D), with quantitative analysis corroborating these observations (bottom panel; Fn/c of 1.0 and 4.5 for cell expressing control RNAi and exportin 1 CRM1 RNAi respectively). Thus, β-DG traffics from the nucleus to cytoplasm in an exportin-1/CRM1-dependent fashion.

The localization of β-DG in the NE [9, 11] as well the presence of the NES in the TM region raised important questions about the mechanism that allows β-DG to be available to be exported by CRM1. Since β-DG localizes to both NE and nucleoplasm, we speculate that solely the nucleoplasmic fraction of β-DG is undergoing nuclear export, while the NE-bound fraction of β-DG is inaccessible to CRM1. To test this hypothesis, C2C12 cells were treated with LMB prior to being fractionated into NE and nucleoplasmic extracts. The cell fractions purity was validated by immunodetection of nucleoplasm (Sp3) and NE (emerin) protein markers. Consistent with our hypothesis, inhibition of nuclear export resulted in accumulation of β-DG in the nucleoplasm; in contrast, β-DG NE levels by contrast, remained unaltered after LMB treatment (Figure 3E).

3.3. *Impaired nuclear export of β*-DG affects the levels and NE targeting of lamin B1 and emerin but not lamin A/C

From the above data, it appears that nuclear levels of β-DG are tightly regulated by the balance of nuclear import/export mechanisms. Therefore, we anticipated that abnormal accumulation of β-DG in the nucleus might alter nuclear envelope organization [9]. To test this hypothesis, we analyzed the impact of β-DG nuclear accumulation on the distribution of NE proteins. To this end, cells were transiently transfected to overexpress GFP-β-DG or its shuttling-defective variant GFP-β-DGNESm. To validate the use of recombinant proteins, we fist ascertained whether GFP-β-DG and GFP-β-DGNESm target to the NE and bind to emerin and lamins A/C and B1, as endogenous nuclear β-DG does [9]. CLSM analysis showed that GFP-β-DG and GFP-β NESm localizes to the cytoplasm and nucleus and exhibited a nuclear ring-like staining that suggest their targeting to the NE (Figure 4A). To confirm this, cells were fractionated into NE lysates and further analyzed by SDS/western blotting. GFP-β-DG and GFP-β-DGNESm were recovered in the NE fraction of these cells, together with the nuclear envelope protein marker emerin. The nucleoplasmic marker Sp3 is absent in the NE extract, which confirmed purity of this fraction (Figure 4B). Consistently, GFP-based IP assays demonstrated that both GFP-β-DG and GFP-β-DGNESm but not GFP alone, pulled down emerin and lamins A/C and B1 with similar efficacy (Figure 4C). Next, we proceeded to analyze the distribution of NE proteins in cells stably expressing the recombinant proteins. Most of the cells expressing either GFP alone or GFP-β-DG displayed the typical ring-like perinuclear labeling for the three NE proteins (Figure 5A), with the exception of some GFP-β-DG-transfected

cells that exhibited a marginal decrease in NE labeling and discrete aggregates outside the nucleus, as we have seen before. Conversely, the majority of cells expressing GFP-β-DGNESm exhibited altered immunostaining for both lamin B1 and emerin, which consist of a marked decrease in the NE staining, with the residual signal localized in discrete aggregates outside the nucleus (Figure 5A). Quantification of cells with emerin/lamin B1 mislocalization confirming these observations (right panels). The distribution of lamin A/C remained largely unaltered in GFP-β-DG NESm-expressing cells suggesting that nuclear accumulation of β-DG affects specifically emerin and lamin B1, as has been seen for nuclear depletion of β-DG [9]. Expression of GFP-β-DGNESm in a transient fashion resulted in a less severe mislocalization and protein aggregation for emerin and lamin B1 (Supplemental Figure. 2). To evaluate whether mislocalization of NE proteins impacts their protein levels, lysates from C2C12 cells stably expressing GFP, GFP-β-DG or GFP-β-DGNESm were analyzed by western blotting with antibodies specific to each NE protein (Figure 5B). Quantitative analysis of immunoblots employing calnexin as loading control, revealed that nuclear accumulation of β-DG resulted in a substantial decrease of lamin B1 (~45%), emerin (~55%) and lamin A (~20%) levels (lower panel). Since the mRNA levels of the NE proteins estimated by RT-qPCR were found to be unaltered in cells stably expressing the shuttling-defective mutant (Figure 5C), it appears that a post-transcriptional mechanism underlies the depletion of emerin, lamin B1 and lamin A levels. This suggests therefore that nuclear accumulated β-DG associates quite strongly with the NE proteins, sufficient to disrupt endogenous NE architecture.

3.4. *Nuclear accumulation of β*-DG compromises emerin-mediated processes

We tested the hypothesis that abnormal nuclear accumulation of β-DG, with concomitant mislocalisation and decreased levels of emerin, might compromise emerin function. Attachment of centrosomes to the outer nuclear membrane has been shown to depend, at least in part, on a microtubule-emerin pathway [27], we therefore analyzed whether expression of the β-DG shuttling-defective mutant affects centrosome linkage to the nucleus (Figure 6A). Interestingly, cells expressing GFP-β-DGNESm exhibited a significant increase in the centrosome-nucleus distance (mean value of 2.811 μm), compared with cells expressing either GFP (mean value of 1.537 μm) or GFP-β-DG (mean value of 1.999 μm). In addition, since emerin promotes nuclear export of β-catenin and thereby down-regulates β-catenin transcriptional activity [28], we examined the distribution and activity of β-catenin in C2C12 cells stably expressing the β-DG shuttling-defective mutant. Levels of nuclear β-catenin were consistently low in control cells expressing either GFP or GFP-β-DG; whereas cells expressing GFP-β-DGNESm with accompanying mislocalization of

emerin, exhibited a more predominant nuclear staining of β-catenin (Figure 6B). To further demonstrate the effect of dystroglycan on stability of emerin, β-catenin transcriptional activity was measured by transfecting a reporter vector in which luciferase expression is controlled by a promoter containing multiple β-catenin-TCF DNA elements (TOPGLOW), with a mutant promoter-containing vector (FLOPGLOW) used as control. We saw a more than 2-fold increase in β-catenin activity in cells expressing GFP-β-DGNESm, compared with control cells (Figure 6C). Overall these data suggest that displacement of emerin from the NE, due to altered nuclear export of β-DG, ultimately undermined secondary functions of emerin including centrosome positioning and control of the transcriptional activity of β-catenin.

3.5. *Expression of the β*-DG shuttling defective mutant impairs lamin B1-dependent processes

Since lamin B1 is crucially involved in cell cycle progression [29], we were prompted to ascertain whether expression of the nuclear export-defective mutant of β-DG leads to an impairment of this process. In keeping with our hypothesis, a marked delay in the growth rate of GFP-β-DGNESm-expressing cells was noted compared to untransfected cells, or cells expressing GFP-β-DG or GFP alone (Figure 7A). The delayed growth rate of GFP-β-DGNESm expressing cells appeared to be due to a delay in G0/G1 phase rather than S-phase, as GFP-β-DGNESm expressing cells showed a significant increase in G0/G1 when released from serum starvation (Figure 7B) whereas when released from thymidine block there was no difference in S phase progression between GFP-β-DGNESm and GFP-β-DG or GFP expressing cells (Figure 7C). Lamin B1 is also involved in the maintenance of nucleolar architecture [30] then, C2C12 cells were arrested in late G1/early S phase by double thymidine treatment (Figure 7D), prior to evaluate the nucleolar structure. Consistent with the ability of β-dystroglycan to affect lamin B1 localisation, increased nuclear accumulation of GFP-β-DG NESm resulted in disaggregation of nucleoli into more numerous and smaller bodies as determined by immunostaining for the nucleolar protein fibrillarin. This was further confirmed by both 3-D reconstruction of nucleoli structure (Figure 7E) and estimation of nucleoli number and nucleolar volume (Figure 7F). These data demonstrate that hindering β-DG nuclear export, with concomitant alteration of lamin B1 localization and expression, results in altered cell cycle progression and distorted nucleolar organization.

3.6. *Forced nuclear accumulation of β*-DG enhances its proteasomal degradation in the nucleus

The lifespan of β-DG has been shown to be modulated by phosphorylation-dependent proteosomal degradation [31]. Therefore we were prompted to analyze whether β-DG stability depends on its subcellular compartmentalization. C2C12 cells were pretreated with leptomycin B (LMB) prior to

inhibiting protein synthesis with cycloheximide, to analyze whether nuclear accumulation of β-DG affects its turnover. Interestingly, we observed a drastic reduction of 50% in the half-live of β-DG upon LMB treatment (Figure 8A) and this decrease in the protein levels was reversed after MG132 treatment (Figure 8B), suggesting that β-DG is more prone to proteosomal degradation within the nucleus. Because ubiquitination is an essential step for further degradation by the proteasome, we monitored the ubiquitination of β-DG in both the cytoplasm and the nucleus. C2C12 lysates were subjected to pulldown with GST-MultiDsk a GST protein fused to 3 repeated ubiquitin binding domains [20]. A higher molecular weight band that is likely to correspond to ubiquitinated β-DG was pulled down by the MultiDsk protein in both cytoplasm and the nucleus, but it was only recognised by the antibody raised against tyrosine phosphorylated β-dystroglycan and not by the antibody that detects unphosphorylated dystroglycan (Figure 8C). Thus, as has been described previously [31], it is only the tyrosine phosphorylated form of β-DG that is ubiquitinated. It is noteworthy that in this study, virtually all nuclear pβ-DG was found to be ubiquitinated in the LMB-treated cells (compare S to P fractions), suggesting a more active ubiquitination of β-DG is in these cells. Overall these data imply that β-DG is degraded by both the cytoplasmic and the nuclear proteasome and that forced nuclear accumulation of pβ-DG enhances its nuclear degradation.

4. Discussion

β-dystroglycan (β-DG) is a well characterized component of the dystrophin associated protein complex (DAPC) of the sarcolemma with critical functions in cell adhesion/signaling and cytoskeleton remodeling [3, 5, 6, 32]. More recently, it has also been found to translocate to the nucleus in an importin α2/β1-dependent fashion [7, 8]. In the nucleus, β-DG is thought to assemble with emerin and lamins A/C and B1 and plays a role in regulating nuclear architecture [9]. In this study, we investigated the nuclear export of β-DG and demonstrate for the first time that β-DG is subject to nucleocytoplasmic shuttling with an active exportin1/CRM1-mediated nuclear export pathway that together with its nuclear import serves to tightly regulate the nuclear levels of β-DG. In addition, we provide evidence that control of nuclear β-DG content by both nuclear export and nuclear proteasomal degradation pathways is physiologically relevant to maintain proper nuclear envelope organization and activity.

We identified a consensus hydrophobic nuclear export signal (NES) in the transmembrane region of β-DG. Using site-directed mutagenesis of GFP-β-DGNES fusion proteins we determined that the NES was functional. Nuclear export of β-DG was shown to be dependent on exportin1/CRM1, as demonstrated by: i) the CRM1-specific inhibitor Leptomycin B (LMB) blocked nuclear export of β-

DG in either C2C12 or primary myoblasts; ii) knockdown of exportin/CRM1 expression resulted in nuclear accumulation of both endogenous β-DG and GFP-β-DG fusion protein and iii) specific interaction of β-DG with exportin/CRM1 was revealed by either in vitro pull down assays and GFP-based immunoprecipitation assays in living cells. Overall these results support the notion that nuclear export of β-DG relies on NES motif recognition by exportin1/CRM1. To our knowledge, β-DG represents a unique example of an inner nuclear membrane protein with functional nuclear export pathway. We found that solely the nucleoplasmic fraction of β-DG is undergoing nuclear export, while the NE-bound fraction of β-DG remained inaccessible to CRM1. These results imply the existence of a molecular mechanism enabling β-DG to reach the nucleoplasm to be then accessible to the CRM1 nuclear export machinery. Elucidation of such mechanisms clearly requires further investigation [33].

Dystroglycan has multiple cellular roles involved in cell adhesion, cell signaling and organization of the cytoskeleton [2]. The spatial and temporal segregation of these multiple activities at the plasma membrane is under tight control, including by tyrosine phosphorylation, ubiquitination and regulated proteolysis [34-37] and through its association with a number of different cytolinker proteins depending on context [2]. Perturbations in dystroglycan homeostasis are evident in diseases such as muscular dystrophies [38] and cancer [39]. Moreover experimental manipulation of cellular dystroglycan levels by RNAi-mediated knockdown or overexpression can have both loss of function and gain of function consequences for cell adhesion, cell migration, cell invasion, anchorage independent growth and cytoskeletal organization [6, 36, 40]. The targeting of dystroglycan to different cellular compartments also impacts on function. Tyrosine phosphorylation of dystroglycan results in internalization of β-DG from the plasma membrane to the cytosol, where it can be targeted to endosomes [35, 41]. We recently demonstrated that β-DG undergoes retrograde trafficking from the PM to the nucleus, via the endosome-endoplasmic reticulum (ER) network. With the assistance of Sec61 β-DG is able to exit the ER membrane and becomes accessible for importin-mediated nuclear import through the nuclear pore [33]. Alternatively, we propose that β-DG transits by lateral movement from ER to the NE, where the Sec61 localized in the NE could mediate the translocation of a fraction of β-DG to the nucleoplasm. Consistent with this paradigm, we show here that aberrant nuclear accumulation of β-DG, through overexpression of a shuttling-defective mutant, has a dominant effect resulting in the mislocalization of the NE proteins emerin and lamin B1. Both proteins lose their characteristic ring-like immunostaining at the NE and accumulate in patches/aggregates localized outside the nucleus. Mistargeting of lamin B1 and emerin is accompanied by reduced protein stability as demonstrated by a decrease in their protein levels but with no change at the transcriptional level. Altered complex topology might impair lamin

B1 and emerin stability by exposing degradation signals that should normally be hidden, making these proteins more accessible to proteosomal attack. Likewise, altered complex structure might lead to lamin B1 and emerin cytoplasmic aggregation through unmasking of aggregation-prone regions. Consistent with this notion, there is growing evidence showing that proper engagement of a protein into a complex increases its stability [42, 43].

The tight regulation of dystroglycan function therefore extends to the nuclear compartment, as either nuclear accumulation (shown here by blocking nuclear export) or nuclear depletion of β-DG [9] leads to aberrant nuclear architecture. It is likely that an excess of nuclear β-DG results in competition between lamin B1 and emerin possibly leading to non-functional pairwise interactions with β-DG rather than functional three-way interactions, whereas sub-stoichiometric levels of β-DG don't allow enough three way interactions to form, the net result in either case being mislocalisation of emerin and lamin B1 and loss of NE architecture (Figure 4). A similar scenario is observed at the sarcolemma where mis-expression of sarcospan, caveolin-3 and plectin leads to competition for binding sites between these proteins and dystroglycan and dystrophin [44-46]. The nuclear accumulation of β-DG disturbs emerin- and lamin B1-dependent functions (Figure 6-7). A significant percentage of C2C12 myoblasts containing high concentration of nuclear β-DG exhibited centrosomes that were detached from the NE, implying that the microtubule-emerin pathway that controls anchorage of centrosomes to the ONM [27] was disrupted in these cells. Furthermore, transcriptional activity of β-catenin, which is partially dependent on emerin-mediated nuclear export of β-catenin [28], was increased in cells containing an excess of nuclear β-DG. In the same way, we found impairment in the lamin B1 activities that control cell cycle progression and nucleoli structure in response to high levels of nuclear β-DG. These cells accumulate at G0/G1 and exhibited delay transition through S phase, which is consistent with a previous study showing prolonged S phase in colon cancer cells with depleted levels of lamin B1[29]. Interestingly the same effect on the cell cycle is seen in Swiss 3T3 cells depleted for dystroglycan [47]. With respect to the nucleolar compartment, we observed the appearance of dispersed and distorted nucleoli concomitant with the nuclear accumulation of β-DG. This is probably due to the role of lamin B1 in modulating nucleoli organization and plasticity [30], it is likely that nuclear overexpression of β-DG impacts nucleoli structure by a primary effect upon lamin B1 expression, localization, interactions and stability. Altogether, these data demonstrate that dysregulation of β-DG nuclear trafficking has physiological consequences on NE organization and activity. In keeping with this idea, cells treated with LMB exhibited accelerated turnover of nuclear β-DG, by nuclear proteosomal degradation, which suggests the activation of alternative protective mechanisms to restrict the lifespan of nuclear β-DG and prevent its harmful accumulation.

It has been observed previously that alterations in the protein levels of one NE component, either by knockdown or overexpression can have deleterious effects on other NE components with which it interacts, with functional and pathological consequences [48]. Lamin B1 overexpression in oligodendrocytes resulted in both altered localization and protein levels of LAP2 (Lamina-Associated Polypeptide 2) and decreased nuclear import of Nup153. [49]. Dosage-sensitivity of the lamin B1-containing NE network is highlighted by the fact that adult-onset autosomal dominant leukodystrophy (disorder characterized by central nervous system demyelination) is caused by lamin B1 overexpression, due to LMNB1 gene duplication [50, 51]. In opposite way, lamin B1 knockdown induced cell senescence in human fibroblasts [52]. Furthermore, either overexpression or downregulation of LUMA (transmembrane protein 43) has a drastic effect on NE structure via mislocalization of emerin [53]. Likewise, decreased emerin levels by antisense treatment resulted in altered centrosome-nucleus distance [27]. Finally, nuclear accumulation of RAC1 (member of the Rho family of small GTPases that localizes in the NE) due to an alteration in its nuclear export pathway, leads to actin polymerization-dependent alterations in NE organization, including aberrant nuclear shape and mislocalization of lamin A/C and emerin, and ultimately to acquisition of a cell invasive phenotype [54]. Therefore, by similar mechanisms, changes in dystroglycan through altered nuclear trafficking, lead to alterations in nuclear architecture.

Several transmembrane surface receptors are known to translocate to the nucleus, either in whole or in part. Cleavage of the intracellular domain (ICD) of several adhesion receptors, such as notch and CD44 and the translocation of the ICD to the nucleus is an integral part of their signalling mechanism. Like β-dystroglycan, the ICD of notch and CD44 have roles in regulating transcriptional activity in the nucleus [55-57]. Tyrosine kinase receptors such as EGFR and FGFR, and GPCRs like the bradykinin B2 receptor are translocated to the nucleus intact [58-62]. The role of the FGFR in the nucleus remains unclear, whereas translocation of the EGFR and bradykinin B2 receptors to the nucleus are believed to also have a role in transcriptional regulation [63, 64]. But unusually β-dystroglycan is also translocated to the nucleus intact, where it functions in the NE as a nuclear cytoskeletal anchor, in a manner similar to its role in the plasma membrane [2]. Possibly, because of the dual role that β-dystroglycan plays in the plasma membrane and the NE, and the fact that β-dystroglycan translocates from plasma membrane to nucleus where increased levels of dystroglycan can have deleterious effects, as we have shown here, β-dystroglycan is also actively degraded or exported from the nucleus. The mechanism of export involves the normal nuclear export pathway via CRM1, but somewhat unusually involves an NES that is part of the transmembrane region of dystroglycan. However, such a mechanism is not without precedent.

Experiments conducted by Myers and colleagues [65], demonstrated a role for the transmembrane region of FGFR in nucleo-cytoplasmic shuttling. Moreover, reviewing their data in the context of current understanding of NES [66], it seems clear that nuclear accumulation of FGFR mutants they generated is due to alteration of a putative NES in the transmembrane region of FGFR1 (^{385}-L I S C M V C S V I V-^{396}) [65]. Thus, our findings demonstrate for the first time a dual role for a cell adhesion receptor acting as a membrane-cytoskeletal anchor in both the plasma membrane and the inner nuclear membrane. The function of β-dystroglycan in both compartments is maintained by tight control of the nucleo-cytoplasmic shuttling of dystroglycan in order to maintain effective interactions with binding partners at the two membrane cytoskeleton interfaces. This presents a new paradigm for the dual function and regulation of an integral membrane protein in both plasma membrane and inner nuclear membrane. Therefore, dysregulation of the β-DG cellular trafficking might have pathological consequences. At this respect, we recently found that overexpression of CRM1 (a hallmark of a large variety of tumors) resulted in β-DG nuclear depletion in prostate cancer cells (unpublished data), which in turn might be related to the aberrant nuclear morphology exhibit by these cells.

In conclusion, we show that β-DG is a nucleus/cytoplasm shuttling protein with a functional nuclear export pathway that depends on the recognition of a NES localized in its transmembrane domain by exportin/CRM1. Remarkably, exportin 1/CRM1 nuclear export and nuclear proteasomal degradation pathways contribute both to control β-DG nuclear content, in order to preserve the structure and functioning of the NE (Figure 9).

5. References

1. Ervasti, J.M. and K.P. Campbell, *A role for the dystrophin-glycoprotein complex as a transmembrane linker between laminin and actin.* J Cell Biol, 1993. **122**(4): p. 809-23.
2. Moore, C.J. and S.J. Winder, *Dystroglycan versatility in cell adhesion: a tale of multiple motifs.* Cell Commun Signal, 2010. **8**: p. 3.
3. Spence, H.J., et al., *Ezrin-dependent regulation of the actin cytoskeleton by beta-dystroglycan.* Hum Mol Genet, 2004. **13**(15): p. 1657-68.
4. Martinez-Zarate, A.D., et al., *Dystroglycan depletion inhibits the functions of differentiated HL-60 cells.* Biochem Biophys Res Commun, 2014. **448**(3): p. 274-80.
5. Spence, H.J., et al., *Dystroglycan, a scaffold for the ERK-MAP kinase cascade.* EMBO Rep, 2004. **5**(5): p. 484-9.
6. Thompson, O., et al., *Modulation of cell spreading and cell-substrate adhesion dynamics by dystroglycan.* J Cell Sci, 2010. **123**(Pt 1): p. 118-27.
7. Lara-Chacon, B., et al., *Characterization of an Importin alpha/beta-recognized nuclear localization signal in beta-dystroglycan.* J Cell Biochem, 2010. **110**(3): p. 706-17.

8. Oppizzi, M.L., et al., *Nuclear translocation of beta-dystroglycan reveals a distinctive trafficking pattern of autoproteolyzed mucins.* Traffic, 2008. **9**(12): p. 2063-72.
9. Martinez-Vieyra, I.A., et al., *A role for beta-dystroglycan in the organization and structure of the nucleus in myoblasts.* Biochim Biophys Acta, 2013. **1833**(3): p. 698-711.
10. Das, M., et al., *Differentiation of skeletal muscle and integration of myotubes with silicon microstructures using serum-free medium and a synthetic silane substrate.* Nat Protoc, 2007. **2**(7): p. 1795-801.
11. Gonzalez-Ramirez, R., et al., *Nuclear and nuclear envelope localization of dystrophin Dp71 and dystrophin-associated proteins (DAPs) in the C2C12 muscle cells: DAPs nuclear localization is modulated during myogenesis.* J Cell Biochem, 2008. **105**(3): p. 735-45.
12. Schindelin, J., et al., *Fiji: an open-source platform for biological-image analysis.* Nat Methods, 2012. **9**(7): p. 676-82.
13. Rivier, F., et al., *Utrophin and dystrophin-associated glycoproteins in normal and dystrophin deficient cardiac muscle.* J Muscle Res Cell Motil, 1999. **20**(3): p. 305-14.
14. Ilsley, J.L., M. Sudol, and S.J. Winder, *The WW domain: linking cell signalling to the membrane cytoskeleton.* Cell Signal, 2002. **14**(3): p. 183-9.
15. Pereboev, A.V., et al., *Epitopes in the interacting regions of beta-dystroglycan (PPxY motif) and dystrophin (WW domain).* Biochim Biophys Acta, 2001. **1527**(1-2): p. 54-60.
16. Cronshaw, J.M., et al., *Proteomic analysis of the mammalian nuclear pore complex.* J Cell Biol, 2002. **158**(5): p. 915-27.
17. Matunis, M.J., *Isolation and fractionation of rat liver nuclear envelopes and nuclear pore complexes.* Methods, 2006. **39**(4): p. 277-83.
18. Qi, M.L., et al., *Proteome analysis of soluble nuclear proteins reveals that HMGB1/2 suppress genotoxic stress in polyglutamine diseases.* Nat Cell Biol, 2007. **9**(4): p. 402-14.
19. Aguilar, A., et al., *Nuclear localization of the dystrophin-associated protein alpha-dystrobrevin through importin alpha2/beta1 is critical for interaction with the nuclear lamina/maintenance of nuclear integrity.* FASEB J, 2015. **29**(5): p. 1842-58.
20. Wilson, M.D., et al., *MultiDsk: a ubiquitin-specific affinity resin.* PLoS One, 2012. **7**(10): p. e46398.
21. Yashiroda, Y. and M. Yoshida, *Nucleo-cytoplasmic transport of proteins as a target for therapeutic drugs.* Curr Med Chem, 2003. **10**(9): p. 741-8.
22. Cook, A., et al., *Structural biology of nucleocytoplasmic transport.* Annu Rev Biochem, 2007. **76**: p. 647-71.
23. Hutten, S. and R.H. Kehlenbach, *CRM1-mediated nuclear export: to the pore and beyond.* Trends Cell Biol, 2007. **17**(4): p. 193-201.
24. la Cour, T., et al., *NESbase version 1.0: a database of nuclear export signals.* Nucleic Acids Res, 2003. **31**(1): p. 393-6.
25. Henry, M.D. and K.P. Campbell, *Dystroglycan: an extracellular matrix receptor linked to the cytoskeleton.* Curr Opin Cell Biol, 1996. **8**(5): p. 625-31.
26. Ishizawa, J., et al., *Expression, function, and targeting of the nuclear exporter chromosome region maintenance 1 (CRM1) protein.* Pharmacol Ther, 2015. **153**: p. 25-35.
27. Salpingidou, G., et al., *A novel role for the nuclear membrane protein emerin in association of the centrosome to the outer nuclear membrane.* J Cell Biol, 2007. **178**(6): p. 897-904.
28. Markiewicz, E., et al., *The inner nuclear membrane protein emerin regulates beta-catenin activity by restricting its accumulation in the nucleus.* Embo j, 2006. **25**(14): p. 3275-85.
29. Camps, J., et al., *Loss of lamin B1 results in prolongation of S phase and decondensation of chromosome territories.* FASEB J, 2014. **28**(8): p. 3423-34.

30. Martin, C., et al., *Lamin B1 maintains the functional plasticity of nucleoli.* J Cell Sci, 2009. **122**(Pt 10): p. 1551-62.
31. Lipscomb, L., et al., *Dasatinib as a treatment for Duchenne muscular dystrophy.* Hum Mol Genet, 2016. **25**(2): p. 266-74.
32. Chen, Y.J., et al., *Direct interaction of beta-dystroglycan with F-actin.* Biochem J, 2003. **375**(Pt 2): p. 329-37.
33. Gracida-Jiménez V, M.-G.R., Vélez-Aguilera G, Vásquez-Limeta A, Laredo-Cisneros MS, Gómez-López J, Vaca L, Gourlay SC, Jacobs LA, Winder SJ and Cisneros B, *Retrograde trafficking of β-dystroglycan from the plasma membrane to the nucleus* in *Scientific Reports* 2017.
34. James, M., et al., *Adhesion-dependent tyrosine phosphorylation of (beta)-dystroglycan regulates its interaction with utrophin.* J Cell Sci, 2000. **113 (Pt 10)**: p. 1717-26.
35. Miller, G., et al., *Preventing phosphorylation of dystroglycan ameliorates the dystrophic phenotype in mdx mouse.* Hum Mol Genet, 2012. **21**(20): p. 4508-20.
36. Mitchell, A., et al., *Dystroglycan function is a novel determinant of tumor growth and behavior in prostate cancer.* Prostate, 2013. **73**(4): p. 398-408.
37. Leocadio, D., A. Mitchell, and S.J. Winder, *gamma-Secretase Dependent Nuclear Targeting of Dystroglycan.* J Cell Biochem, 2016. **117**(9): p. 2149-57.
38. Riemersma, M., et al., *Absence of alpha- and beta-dystroglycan is associated with Walker-Warburg syndrome.* Neurology, 2015. **84**(21): p. 2177-82.
39. Mathew, G., et al., *Nuclear targeting of dystroglycan promotes the expression of androgen regulated transcription factors in prostate cancer.* Sci Rep, 2013. **3**: p. 2792.
40. Batchelor, C.L., et al., *Recruitment of Dbl by ezrin and dystroglycan drives membrane proximal Cdc42 activation and filopodia formation.* Cell Cycle, 2007. **6**(3): p. 353-63.
41. Sotgia, F., et al., *Localization of phospho-beta-dystroglycan (pY892) to an intracellular vesicular compartment in cultured cells and skeletal muscle fibers in vivo.* Biochemistry, 2003. **42**(23): p. 7110-23.
42. Buchler, N.E., U. Gerland, and T. Hwa, *Nonlinear protein degradation and the function of genetic circuits.* Proc Natl Acad Sci U S A, 2005. **102**(27): p. 9559-64.
43. Tompa, P., et al., *Structural disorder serves as a weak signal for intracellular protein degradation.* Proteins, 2008. **71**(2): p. 903-9.
44. Miller, G., et al., *Structural and functional analysis of the sarcoglycan-sarcospan subcomplex.* Exp Cell Res, 2007. **313**(4): p. 639-51.
45. Galbiati, F., B. Razani, and M.P. Lisanti, *Caveolae and caveolin-3 in muscular dystrophy.* Trends Mol Med, 2001. **7**(10): p. 435-41.
46. Rezniczek, G.A., et al., *Plectin 1f scaffolding at the sarcolemma of dystrophic (mdx) muscle fibers through multiple interactions with beta-dystroglycan.* J Cell Biol, 2007. **176**(7): p. 965-77.
47. Higginson, J.R., O. Thompson, and S.J. Winder, *Targeting of dystroglycan to the cleavage furrow and midbody in cytokinesis.* Int J Biochem Cell Biol, 2008. **40**(5): p. 892-900.
48. Meinke, P. and E.C. Schirmer, *The increasing relevance of nuclear envelope myopathies.* Curr Opin Neurol, 2016. **29**(5): p. 651-61.
49. Lin, S.T. and Y.H. Fu, *miR-23 regulation of lamin B1 is crucial for oligodendrocyte development and myelination.* Dis Model Mech, 2009. **2**(3-4): p. 178-88.
50. Padiath, Q.S., et al., *Lamin B1 duplications cause autosomal dominant leukodystrophy.* Nat Genet, 2006. **38**(10): p. 1114-23.
51. Dos Santos, M.M., et al., *Adult-onset autosomal dominant leukodystrophy due to LMNB1 gene duplication.* J Neurol, 2012. **259**(3): p. 579-81.

52. Shah, P.P., et al., *Lamin B1 depletion in senescent cells triggers large-scale changes in gene expression and the chromatin landscape.* Genes Dev, 2013. **27**(16): p. 1787-99.
53. Bengtsson, L. and H. Otto, *LUMA interacts with emerin and influences its distribution at the inner nuclear membrane.* J Cell Sci, 2008. **121**(Pt 4): p. 536-48.
54. Navarro-Lerida, I., et al., *Rac1 nucleocytoplasmic shuttling drives nuclear shape changes and tumor invasion.* Dev Cell, 2015. **32**(3): p. 318-34.
55. Kidd, S., T. Lieber, and M.W. Young, *Ligand-induced cleavage and regulation of nuclear entry of Notch in Drosophila melanogaster embryos.* Genes Dev. , 1998. **12**(23): p. 3728-3740.
56. Schroeter, E.H., J.A. Kisslinger, and R. Kopan, *Notch-1 signalling requires ligand-induced proteolytic release of intracellular domain.* Nature, 1998. **393**(6683): p. 382-6.
57. Okamoto, I., et al., *Proteolytic release of CD44 intracellular domain and its role in the CD44 signaling pathway.* J. Cell Biol., 2001. **155**: p. 755-762.
58. Lin, S.Y., et al., *Nuclear localization of EGF receptor and its potential new role as a transcription factor.* Nat Cell Biol, 2001. **3**(9): p. 802-8.
59. Maher, P.A., *Nuclear Translocation of fibroblast growth factor (FGF) receptors in response to FGF-2.* J Cell Biol, 1996. **134**(2): p. 529-36.
60. Prudovsky, I.A., et al., *The nuclear trafficking of extracellular fibroblast growth factor (FGF)-1 correlates with the perinuclear association of the FGF receptor-1alpha isoforms but not the FGF receptor-1beta isoforms.* J Biol Chem, 1996. **271**(24): p. 14198-205.
61. Stachowiak, M.K., et al., *Nuclear accumulation of fibroblast growth factor receptors is regulated by multiple signals in adrenal medullary cells.* Mol Biol Cell, 1996. **7**(8): p. 1299-317.
62. Lee, D.K., et al., *Agonist-independent nuclear localization of the Apelin, angiotensin AT1, and bradykinin B2 receptors.* J Biol Chem, 2004. **279**(9): p. 7901-8.
63. Savard, M., et al., *Expression of endogenous nuclear bradykinin B2 receptors mediating signaling in immediate early gene activation.* J Cell Physiol, 2008. **216**(1): p. 234-44.
64. Wang, Y.N., et al., *Nuclear trafficking of the epidermal growth factor receptor family membrane proteins.* Oncogene, 2010. **29**(28): p. 3997-4006.
65. Myers, J.M., et al., *Nuclear trafficking of FGFR1: a role for the transmembrane domain.* J Cell Biochem, 2003. **88**(6): p. 1273-91.
66. Kosugi, S., et al., *Nuclear export signal consensus sequences defined using a localization-based yeast selection system.* Traffic, 2008. **9**(12): p. 2053-62.

FIGURE LEGENDS

Figure 1. **Nucleocytoplasmic shuttling of β-DG in C2C12 and primary mouse myoblasts is prevented by LMB.** (A) LMB treatment effectively blocks the CRM1-mediated nuclear export of GFP-NESRev. C2C12 myoblasts transiently expressing GFP-NESRev protein were used to demonstrate the efficiency of LMB in blocking nuclear export. Cells treated with LMB (inhibitor of exportin CRM1) or vehicle alone (see Methods) were subjected to CLSM analysis. Cell were stained with DAPI for nuclei visualization. (B) C2C12 myoblasts were treated with LMB or ethanol 70% (vehicle) and then immunostained for β-DG using the indicated primary anti-β-DG antibodies. Cells were counterstained with DAPI to decorate nuclei, prior to analysis by CLSM. (C) C2C12 cells were transiently transfected to express GFP or GFP-β-DG and 8 h post-transfection and treated with LMB as above. Cells were then stained for actin-based cytoskeleton (Phalloidin; red) and nuclei (DAPI) visualization. Transfected cells were imaged by CLSM. Bottom panel. Quantitative analysis to determine the nuclear to cytoplasmic fluorescence ratio (Fn/c) of GFP and GFP-β-DG was performed using Fiji software. (D) Mouse primary myoblasts were treated with LMB or vehicle alone prior to immunostaining for β-DG and counterstained for F-actin and nuclei, and then subjected to CLSM analysis. Bottom panel. Fn/c ratios of vehicle- and LMB-treated cultures were calculated as above. Data represent means $\pm$SEM of three separate experiments ($n > 50$ cells), with significance denoted by P values (unpaired t test). Subcellular distribution of β-DG is sensitive to LMB. Typical single Z-sections of confocal CLSM images are shown. Scale bar is 10 µm.

Figure 2. **Identification and functional characterization of a nuclear export signal (NES) in β-DG.** (A) Schematic representation of β-DG showing the localization of the NES motif in the context of the transmembrane (TM) domain. Comparison of the putative NES motif of β-DG with a consensus NES motif and its alignment with the corresponding sequences in β-DG orthologous from different species. (B) C2C12 myoblasts transiently expressing GFP or GFP fused to the NES of β-DG (GFP-NES-β-DG) were analyzed by WB using anti-GFP antibodies. (C) C2C12 myoblasts were transfected to express GFP or GFP-NES-β-DG and 12 h post-transfection incubated with LMB or vehicle alone (see Methods). Cells were stained with DAPI to visualize nuclei and imaged by CLSM. Scale bar, 10 µm. Right panel. The nuclear to cytoplasmic fluorescence ratio (Fn/c) of GFP and GFP-NES-β-DG in the absence or presence of LMB was determined as described in Figure 1D. Data correspond to mean ±SEM of three separate experiments (n > 50 cells), with a significant difference denoted by P value (unpaired t test). The NES of β-DG shifted the distribution of GFP from the nucleus to the cytoplasm but upon LMB treatment the fusion protein accumulated in the nucleus. (D) Expression of GFP-β-DG or its mutant variant GFP-β-DGNESm were analyzed by SDS-PAGE/WB using anti-GFP antibodies. (E) Cells transiently transfected to express GFP-β-DG or GFP-β-DGNESm and 24 h post-transfection were incubated with LMB or vehicle alone as above. Cells were then fixed, stained with phalloidin and DAPI to decorate actin and nuclei respectively and subjected to CLSM analysis. The hydrophobic residues changed to alanines in the mutated NES are denoted in red. Typical single optical Z-sections of CLSM images are shown; scale bar, 10 µm. Right panel. Fn/c ratios of recombinant proteins were determined as described in C. Data represent mean ±SEM of four separate experiments (n > 50 cells), with significant difference denoted by P value (unpaired t test.).

Figure 3. **Nuclear export of β-DG is dependent on exportin 1/ CRM1.** (A) Bacterially expressed GST and GST-β-DG proteins were visualized by SDS-PAGE (top panel). The interaction between β-DG and exportin 1/CRM was determined by pull down and SDS-PAGE/WB analyses using C2C12 lysates and anti-exportin-1/CRM1 antibodies (bottom panel). Inputs correspond to 5% of extracts prior to pull-down. B, bound fraction; Un, unbound fraction. (B) Binding of β-DG to exportin1/CRM1 in living cells. Lysates from C2C12 myoblasts expressing GFP-β-DG or GFP-β-DGNESm were immunoprecipitated using GFP-trap and precipitated proteins subjected to SDS-PAGE/WB analysis using anti-exportin 1/CRMI or anti-GFP antibodies. Inputs correspond to 5% of lysates prior to immunoprecipitation. B, bound fraction; Un, unbound fraction. (C) C2C12 myoblasts were stably expressing with vector expressing either an irrelevant RNAi (control RNAi) or an RNAi designed against exportin 1/CRM1 mRNA (CRM1 RNAi). Exportin1/CRM1 expression was analyzed by SDS-PAGE/WB using antibodies against exportin 1/CRM1 or actin (loading control). (D) Knockdown of exportin 1/CRM1 expression impairs nuclear export of β-DG. C2C12 myoblasts stably expressing either control or exportin 1/CRM1 RNAi were immunostained for β-DG and counterstained with DAPI for nuclei visualization. CLSM analysis with typical single optical Z-sections shown; scale bar 10 μm. The Fn/c ratio of β-DG (bottom panel) was measured as described in Figure 1D. Data represent mean ±SEM of three independent experiments (n > 50 cells), with P value denoting significant difference (unpaired t test). β-DG nuclear export is mediated by exportin 1/CRM1. (E) Cells, treated with LMB or vehicle alone (ethanol) as in Figure 1, were subjected to cell fractionation to isolate nucleoplasmic and NE extracts. Protein extracts were then analyzed by SDS-PAGE/WB using anti-β-DG antibodies. Stripped membranes were reprobed for Sp3 and emerin, purity controls for nucleoplasm and NE respectively.

Figure 4. **GFP-β-DG and GFP-β-DGNESsm are targeted to the NE and interact with NE proteins.** (A) Distribution of GFP-β-DG and GFP-β-DGNESsm was analyzed by CLSM in C2C12 cells at 24 h post-transfection. Nuclei were decorated by staining with DAPI. Scale bar, 10 μm. (B). C2C12 cell were subjected to cell fractionation to obtain nuclear envelope (NE) fractions respectively. Stripped membranes were reprobed for caveolin 3 (membrane protein), actin (cytoplasmic protein), Sp3 (nucleoplasmic protein) and emerin (NE marker), to demonstrate the cell fractions purity. (C) Interaction of GFP-β-DG and GFP-β-DGNESm with NE proteins was analyzed using the GFP-Trap system. Immunoprecipitated and unbound fractions were analyzed by SDS-PAGE/WB using specific antibodies against lamin B1, lamin A/C, emerin and GFP (control).

Input corresponds to 5% of total lysates prior to immunoprecipitation. B, bound fraction; Un, unbound fraction.

Figure 5. **Overexpression of the β-DG shuttling defective mutant alters the localization and levels of emerin and lamin B1.** (A) C2C12 myoblasts stably expressing GFP, GFP-β-DG or GFP-β-DGNESm, were immunostained for the indicated NE proteins and counterstained with DAPI prior to analysis by CLSM. Typical single optical Z-sections are shown; scale bar 10 µm. The percentage of cells showing altered localization of the indicated NE proteins was calculated (right panels). Results represent mean ±SEM of three independent experiments (n= 100 cells), with P values showing significant differences (unpaired t test). C2C12 myoblasts stably expressing GFP, GFP-β-DG or GFP-β-DGNESm, were subjected to SDSPAGE/western blotting (B) and qRT-PCR (C) analyses. (B) Lysates were analyzed by SDS-PAGE/WB using specific antibodies against lamin B1, lamin A/C, emerin and calnexin (loading control) and their protein levels were measured by densitometry analysis. Results correspond to mean ±SEM of three separate experiments, with P values showing significant differences (unpaired t test). (C) qRT- PCR assays were carried out to measure RNA levels of lamin B1, lamin A/C, emerin or GAPDH (control). The relative levels obtained in cells transfected with GFP alone were set at 1. Data represent mean ±SEM of three separate experiments.

Figure 6. **Defective nuclear-cytoplasmic shuttling of β-DG affects both centrosome positioning and β-catenin signaling.** (A) C2C12 myoblasts stably expressing either GFP, GFP-β-DG or GFP-β-DGNESm were double stained with anti-γ-tubulin antibody and DAPI to decorate centrosomes and nuclei respectively. Typical images showing centrosome positioning are shown; scale bar, 10 µm. Nuclear-centrosome distance, indicated by white lines (lower image), were measured in overlaid images using Leica Application Suite, Advanced Fluorescence Lite imaging processing software. Data from three separate experiments (n=200 cells) are shown in a box-and-whisker plot (bottom panel), with P value indicating significance difference (unpaired t test). (B) Transfected cells were immunostained for β-catenin and counterstained with DAPI to visualize nuclei. (C) Cells were transiently transfected with either GFP, GFP-β-DG or GFP-β-DGNESm, along with TOPFLASH or its mutant promoter variant FLOPFLASH and TK Renilla. After incubation for 24 h the luciferase activity was measured as described in Methods. Control condition (100% of luciferase activity) correspond to the TOPFLASH/FLOPFLASH ratio obtained in cells transfected with GFP alone. Data represent mean

±SEM of three independent experiments; P values denote significant difference (unpaired t test). β-DG nuclear accumulation impaired nuclear functions mediated by emerin.

Figure 7. **Expression of the β-DG shuttling defective mutant alters both cell cycle progression and nucleoli structure.** C2C12 myoblasts that stably expressed GFP, GFP-β-DG or GFP-β-DGNESm were obtained for the following assays. (A) Cell proliferation was monitored over a 14-day period using the MTT assay. Stably expressing cells were synchronized at G0/G1 phase by serum starvation for 48 h (B) or at S phase by thymidine treatment (C) and then released into the cell cycle. Cells were fixed and stained with DAPI to determine DNA content at the indicated times. Cell cycle profiles were analyzed by flow cytometry and their graphical representation correspond to the average percentage of cells at each phase of three independent experiments. (D) Cells were synchronized at S phase by double thymidine treatment prior to the analysis of nucleolar structure (E) Cells were grown on coverslips, immunostained for fibrillarin and further subjected to CLSM to examine nucleolar morphology; scale bar 10 μm. 3D reconstruction of nucleoli was obtained from optical Z-sections (0.4μm step size) using Fiji software. (F) The number of nucleoli per cell (top panel) and the nucleoli volume (bottom panel) were determined in each cell culture (n = 200 cells) using Fiji software. Data from three separate experiments (n=200 cells) are shown in a box-and-whisker plot (bottom panel), with P value indicating significance difference (unpaired t test). β-DG nuclear accumulation altered lamin B1-dependent functions.

Figure 8. **LMB-mediated nuclear accumulation of β-DG accelerates its degradation by the nuclear proteome.** (A) C2C12 myoblasts were treated with LMB or vehicle alone (see methods) and then with CHX for the indicated time intervals. Cell lysates were subjected to SDS-PAGE/WB analysis using specific antibodies for β-DG and GAPDH (loading control). Right panel. β-DG half-life ($t_{1/2}$) was calculated by densitometry analysis of autoradiograms (t0 =100%). Data correspond to mean ±SEM of three separate experiments and the linear regression plot was obtained using Graphpad Prism 6 software. β-DG turnover was accelerated in LMB-treated cells. (B) C2C12 myoblasts treated with LMB and CHX as in (A) were further incubated for 30 h with MG132 (proteasome inhibitor) or vehicle alone. Data correspond to mean ±SEM of three separate experiments, with P value indicating significance differences (unpaired t test). Proteasome inhibition recovered β-DG protein levels. (C) C2C12 cells treated with LMB or vehicle alone for 12h were fractionated into cytoplasmic and nuclear extracts and further subjected to pulldown assay. Supernatant (S) and pellet (P) samples from control Glutathione-S-transferase (GST) and

GST-MultiDsk ubiquitin binding protein pulldown were separated by SDS-PAGE and western blotted for pY892 β-dystroglycan (p-βDG, lower panel) or the unphosphorylated counterpart (β-DG, upper panel). Calnexin and lamin A/C served as cell fractionation purity controls for cytoplasm and nucleus respectively. Nuclear degradation of p-β-DG by the ubiquitin-proteasome pathway was enhanced upon LMB treatment.

Figure 9. **Functional consequences of altered β-DG nuclear export.** (A) The nuclear β-DG content is controlled by CRM1-mediated nuclear export (1) and nuclear proteosomal degradation of phospho-β-DG [Tyr^{892}] (2). (B) Nuclear accumulation of β-DG due to LMB treatment (1) or the expression of a β-DG shuttling-defective mutant (2) resulted in altered NE organization and function. Mislocalization and decreased levels of emerin (3) and lamin B1 (5) resulted in impaired emerin- and lamin B1-dependent functions, including anchorage of the centrosomes to the ONM (4) and maintenance of nucleoli structure (6) respectively. In addition, β-DG nuclear accumulation accelerated degradation of phospho-β-DG by the nuclear proteasome (7).

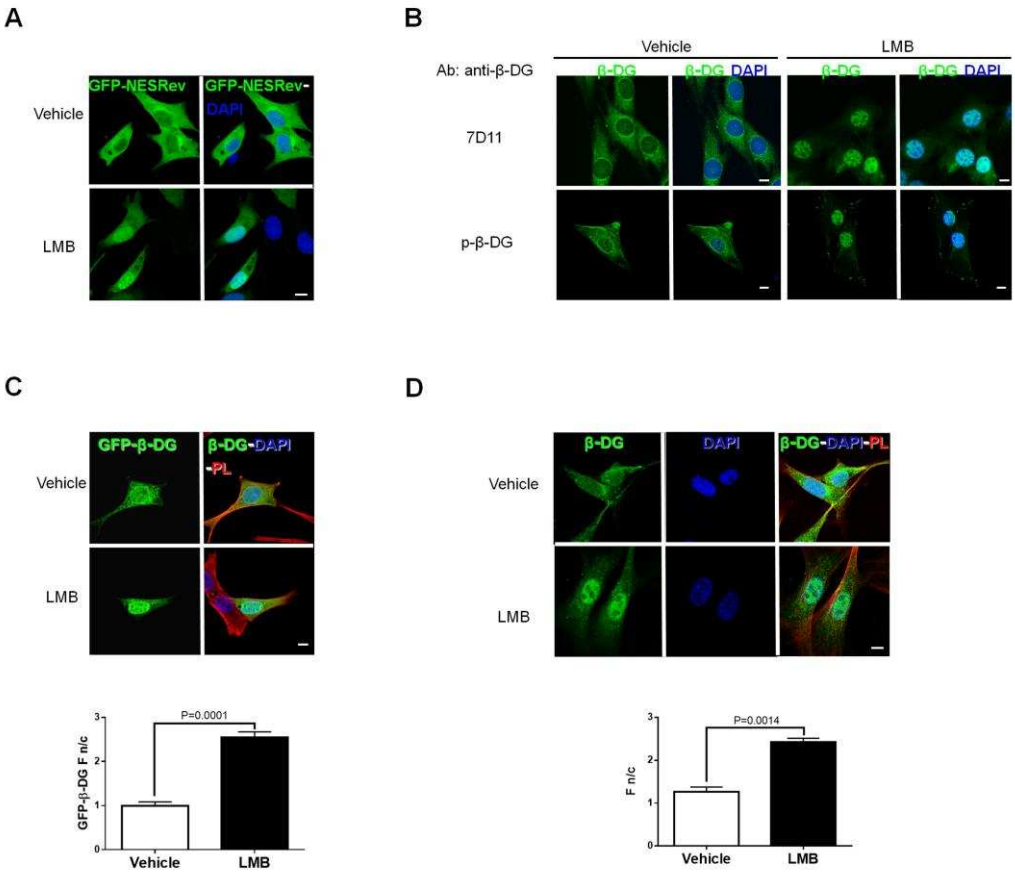

Figure 1

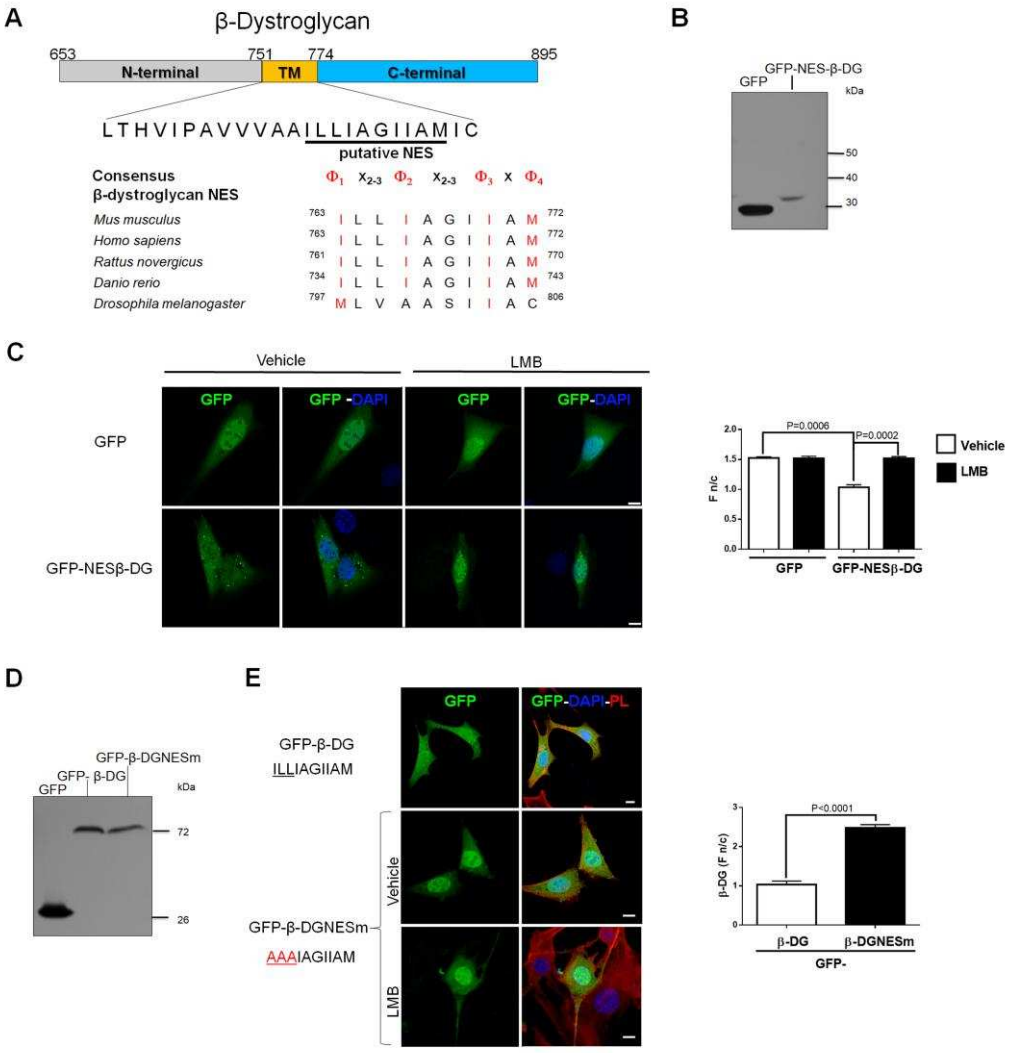

Figure 2

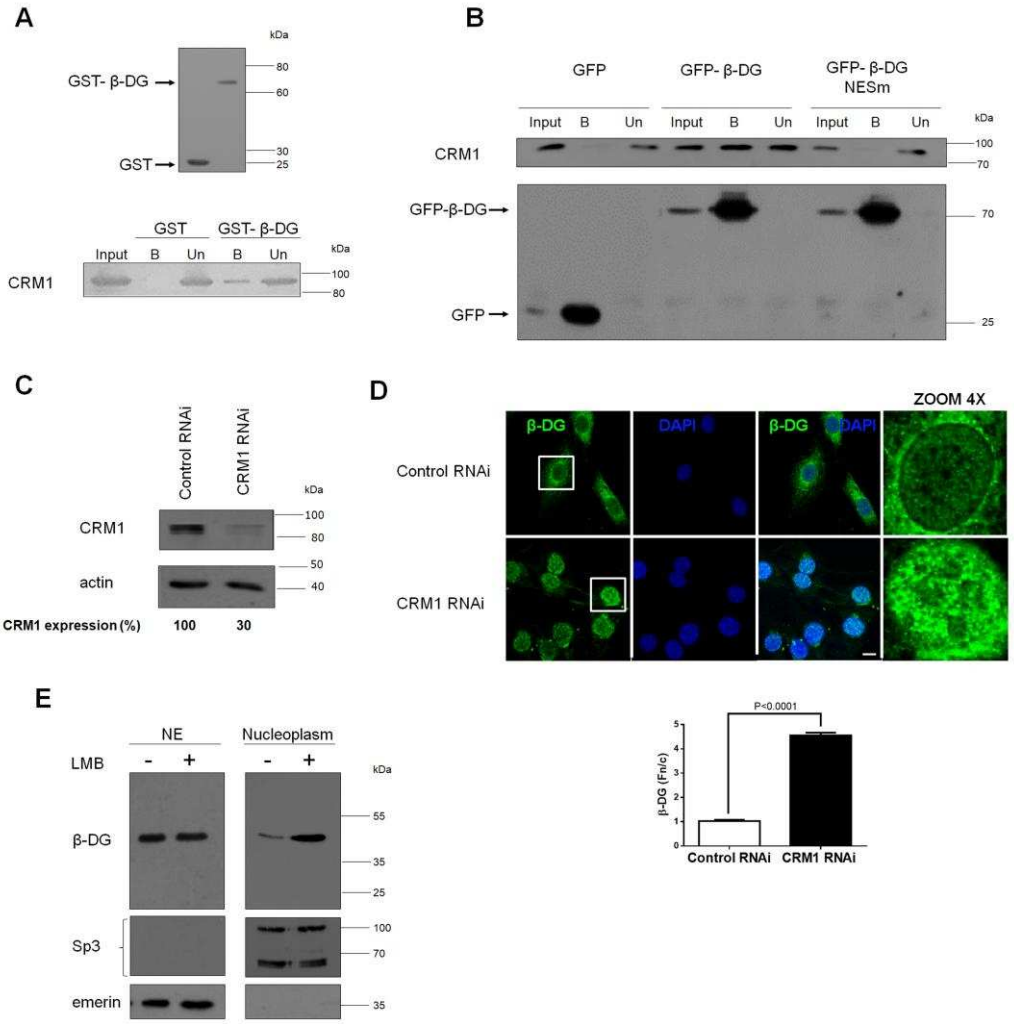

Figure 3

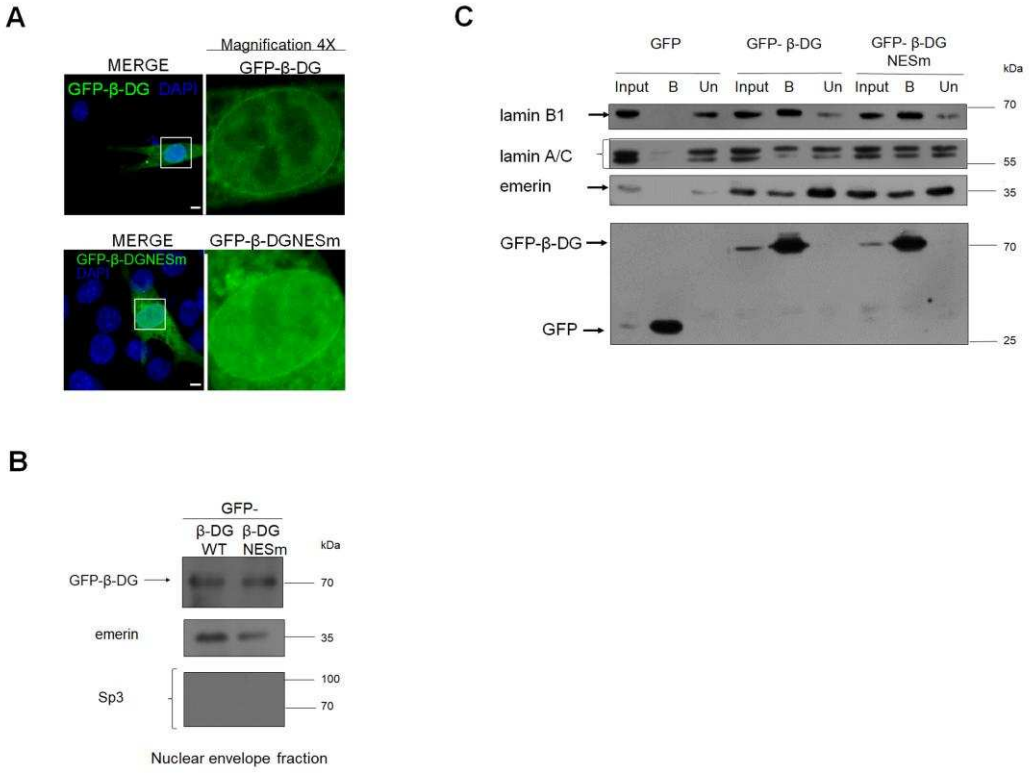

Figure 4

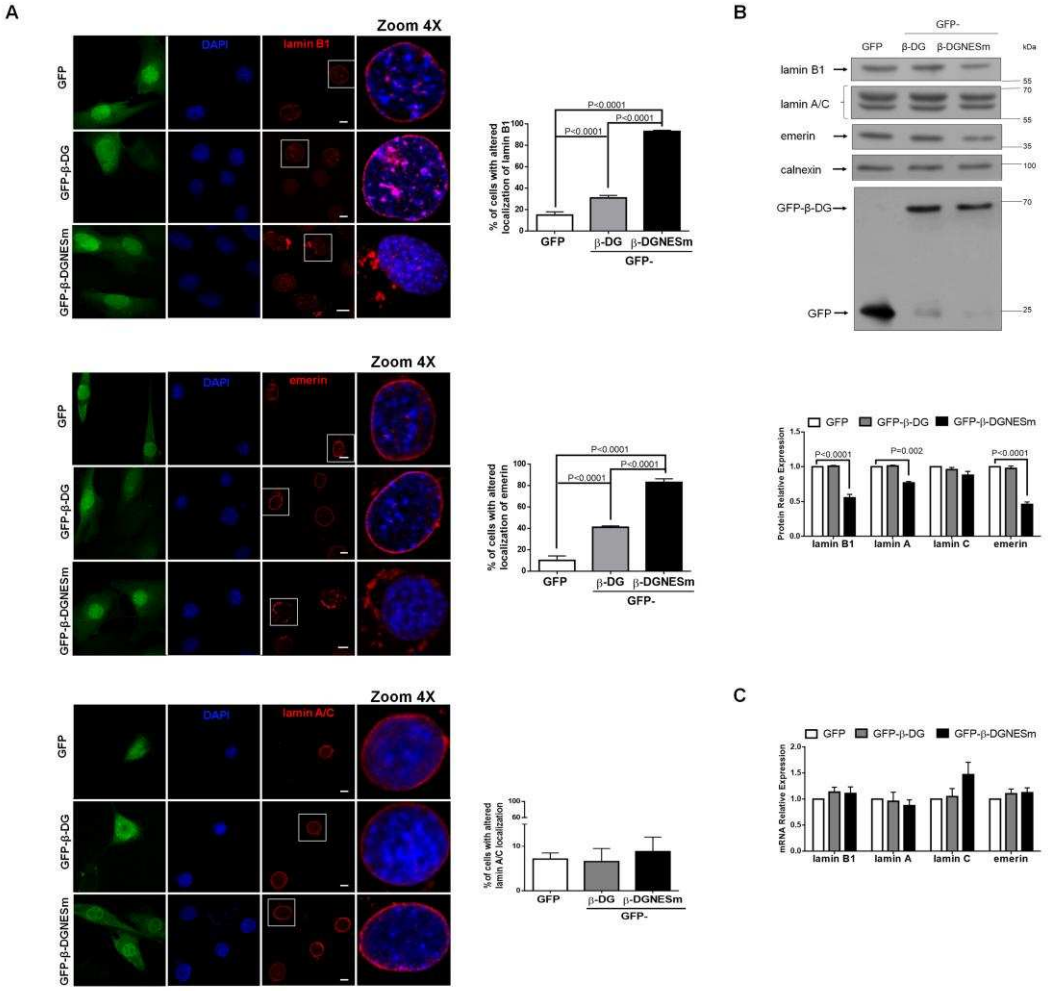

Figure 5

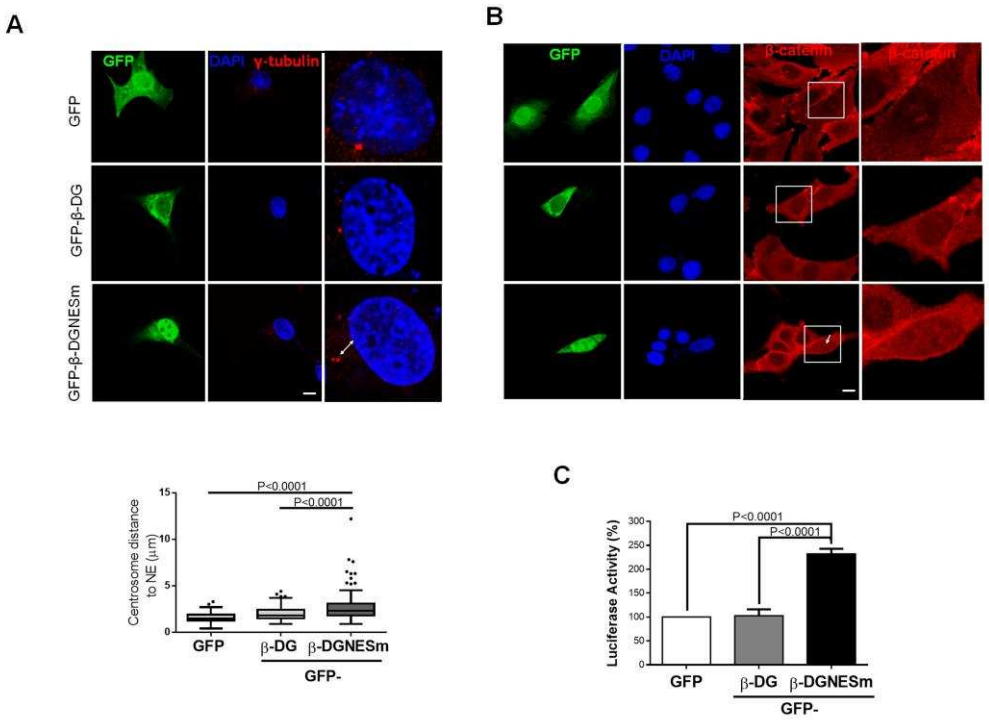

Figure 6

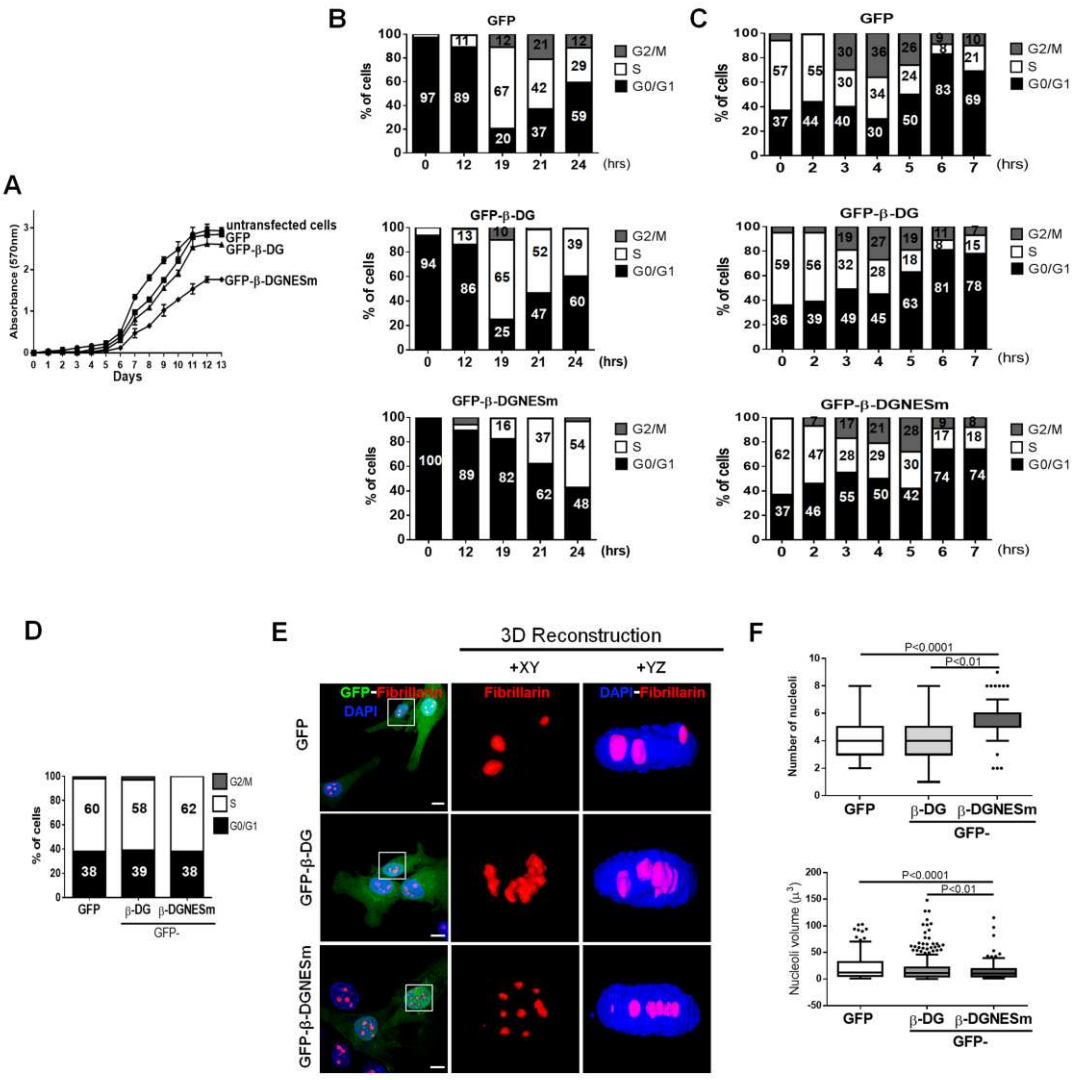

Figure 7

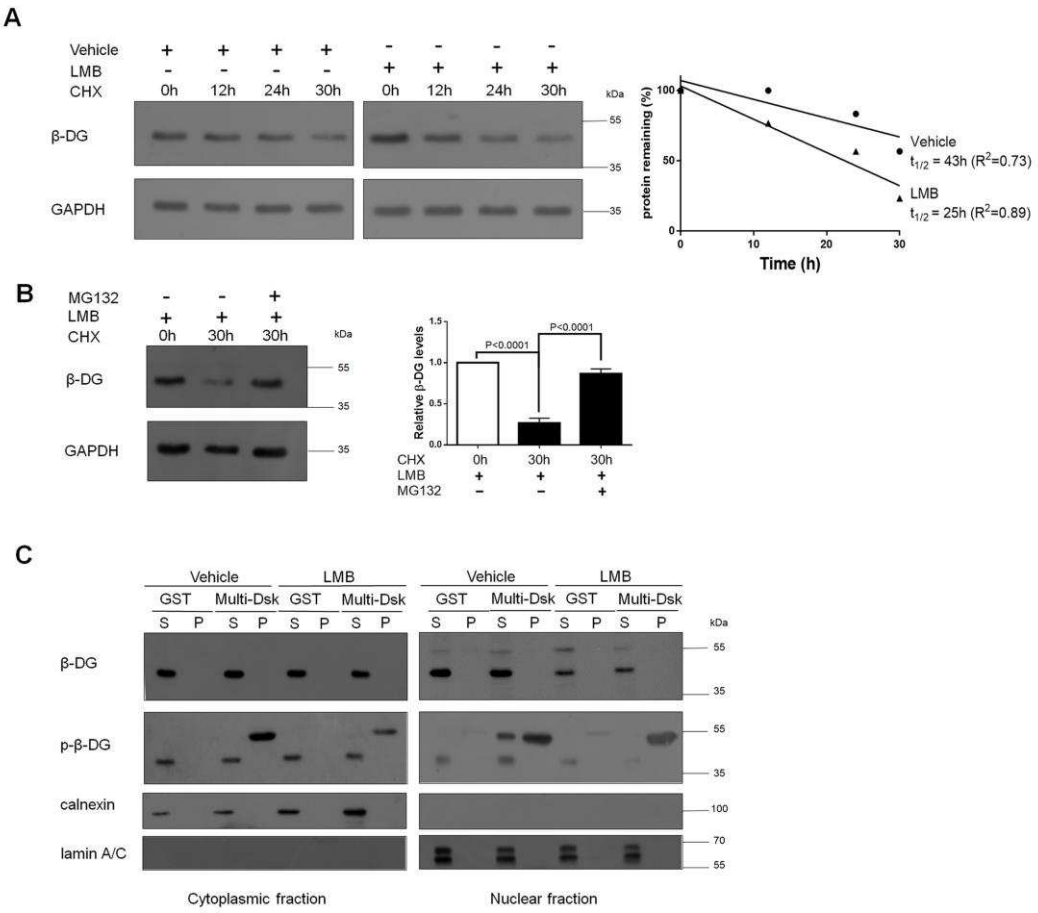

Figure 8

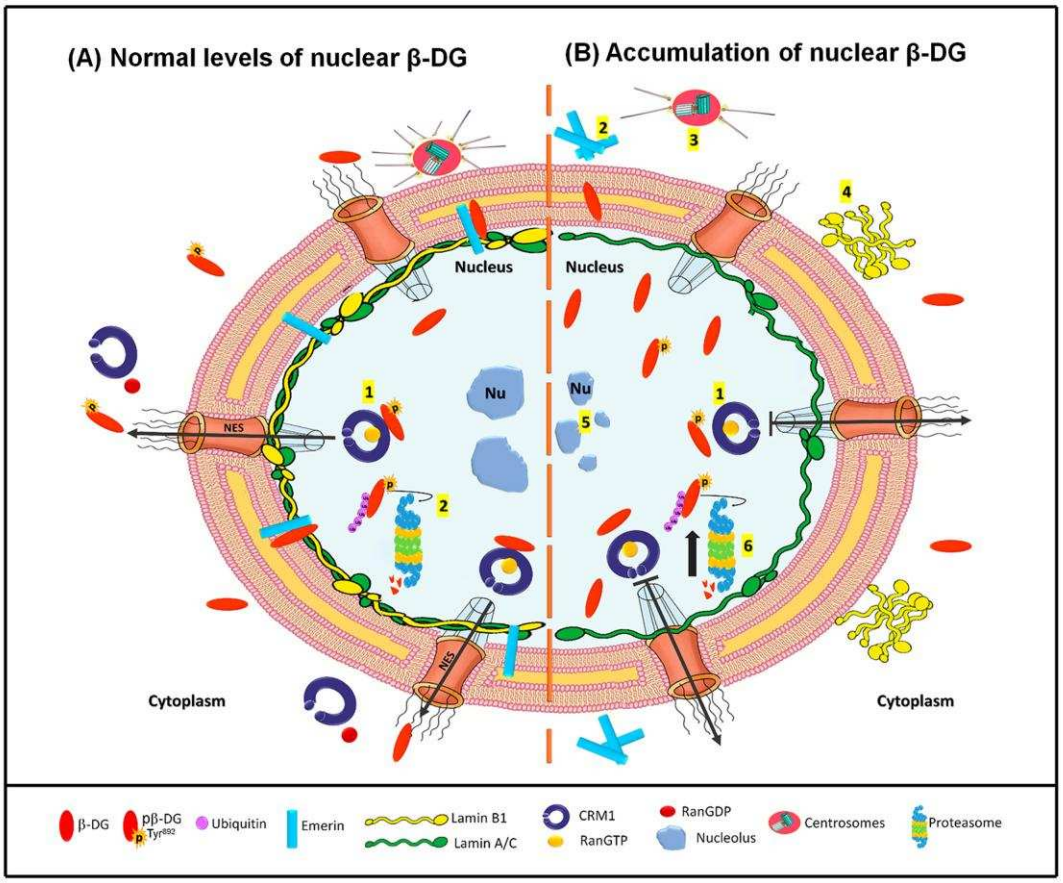

Figure 9

Highlights

- β-dystroglycan possess a functional nuclear export signal in the transmembrane domain.
- Nuclear export of β-dystroglycan is mediated by exportin CRM1.
- Forced nuclear accumulation of β-dystroglycan altered the localization and levels of emerin and lamin B1.
- Nuclear accumulation of β-dystroglycan disrupted nuclear processes in which emerin and lamin B1 are critically involved.
- The nuclear content of β-dystroglycan is regulated by the nuclear export and nuclear proteasome pathways.
- Control of β-dystroglycan nuclear content is crucial for nuclear envelope structure and function.